REPORT DOCUMENTATION PAGE

Form Approved
OMB No. 0704-0188

1. REPORT DATE *(DD-MM-YYYY)*	2. REPORT TYPE	3. DATES COVERED *(From - To)*
03-10-2008	Final report	09/01/2004 - 08/31/2007

4. TITLE AND SUBTITLE
Two-Dimensional Electron Gas in Strained Silicon for Studying Ultra-Low Energy Electronic Processes

5a. CONTRACT NUMBER
FA9550-04-1-0370

5b. GRANT NUMBER

5c. PROGRAM ELEMENT NUMBER

6. AUTHOR(S)
Ya-Hong Xie

Daniel Tsui

5d. PROJECT NUMBER

5e. TASK NUMBER

5f. WORK UNIT NUMBER

7. PERFORMING ORGANIZATION NAME(S) AND ADDRESS(ES)

Dept. Mat. Sci. Eng., University of California
Los Angeles
6532 Boelter Hall, Box 951595
Los Angeles, CA 90095-1595

Department of Electrical Eng
Princeton University

8. PERFORMING ORGANIZATION REPORT NUMBER: 2008 final

9. SPONSORING / MONITORING AGENCY NAME(S) AND ADDRESS(ES)
AFOSR
675 N Randolph St
Arlington VA 22203

10. SPONSOR/MONITOR'S ACRONYM(S)
Dr. Donald Silversmith

11. SPONSOR/MONITOR'S REPORT NUMBER(S)

12. DISTRIBUTION / AVAILABILITY STATEMENT
approved for public release; distribution unlimited;

AFRL-SR-AR-TR-08-0172

13. SUPPLEMENTARY NOTES

20080404105

14. ABSTRACT
The proposed research focuses on the fabrication of high mobility 2D electron gases or low density for the understanding of correlated electron behavior under extreme conditions: low temperature and high magnetic field. The experimental efforts are in 3 related topics: (1) fabricate 2DES in strained Si with the highest achievable electron mobility; (2) fabricate 2DES in strained Si with low electron density; and (3) explore alternative approaches for fabricating strained Si without the relaxed buffer layer that is heavily dislocated and therefore causing strain undulation in the Si channel. Significant progress has been made in carrier mobility and the fabrication of strained films using porous Si. We have gained the ability to reproducibly fabricate 2DES samples with mobility above 300,000 cm2/V-s. By controlled oxidation of porous Si, we have obtained strained films with up to 0.8% tensile strain, suitable for 2DES transport research without ever introducing dislocations. The outcome of our research has led to significant advancement in our ability of fabricating high quality samples for the understanding of correlated electron behavior. .

15. SUBJECT TERMS
2DES, QHE, MIT, strained Si

16. SECURITY CLASSIFICATION OF:			17. LIMITATION OF ABSTRACT	18. NUMBER OF PAGES	19a. NAME OF RESPONSIBLE PERSON
a. REPORT unclassified	b. ABSTRACT unclassified	c. THIS PAGE unclassified	UL	15	Ya-Hong Xie
					19b. TELEPHONE NUMBER *(include area code)* (310) 825-2971

Final Report

Abstract

Our research has been mainly in 3 related topics: (1) fabricate 2DES in strained Si with high electron mobility and fabricate 2DES in strained Si with tailing electron density; and (2) achieve a remarkable strain in Si layer by using porous Si based approach and exploit a new approach to apply uniaxial strain in thin Si layer; and (3) Low-dimensional physics study. Significant progress has been made in all three areas. Our 2DES mobility has been improved from 180,000 cm2/V-s to 350,000 cm2/V-s since the beginning of this program. This mobility can be regarded as the world record of reproducibly achievable mobility. We have also explored one approach to tailoring electron density, which is different from conventional ways of tailoring electron density in the 2DES structure. Secondly, we have successfully achieved 0.8% strain in Si by using a micro-porous Si based approach and we also start to fabricate 2DES structure on porous Si based substrate. In the mean time, we exploit a new method and try to apply uniaxial strain in thin Si layer. We have also demonstrated the feasibility of strained Si fabrication using boro-phosphate silicate based approach that avoids the introduction of dislocation completely. These two approaches have the broader impact of potentially entering the Si VLSI technology. Finally many interesting low-dimensional phenomena were studied on our high quality samples, such as valley splitting, etc.

Detailed Description of Progress

(1) Fabricate 2DES by using MBE approach

1. The improvement for high electron mobility

High electron mobility is one of two important factors have been focused on this research. It is one of the necessary conditions for studying electron-electron interaction under high magnetic field at low temperature. In our case, the electron mobility is mainly limited by the local impurities scattering, which can be greatly reduced by improving the background pressure. During the program period, we have found a tiny leak in our gate valve, which cannot be detected by the conventional leak check using He gas combined with Residual Gas Analysis (RGA). We explored a new method to do the leak check by sealing the gate valve completely with normal plastic bags. These plastic bags are charged with high purity He gas before the sealing. Because there is He gas pressure maintained in the plastic bags, Helium atoms can travel into MBE chamber and detected by RGA; otherwise, the atoms will be pumped out before detected by RGA. After fixing the leak, the background pressure is improved from 2×10^{-9} torr to 2×10^{-11} torr. Therefore, the mobility is almost doubled from 180,000 cm2/V-s to 350,000 cm2/V-s. This mobility is one of the world records for 2DES study. We also established the unique ability to reproducibly fabricate 350,000 cm2/V-s mobility samples with over 70% yield. Figure 1 shows the typical sample structure used in this research.

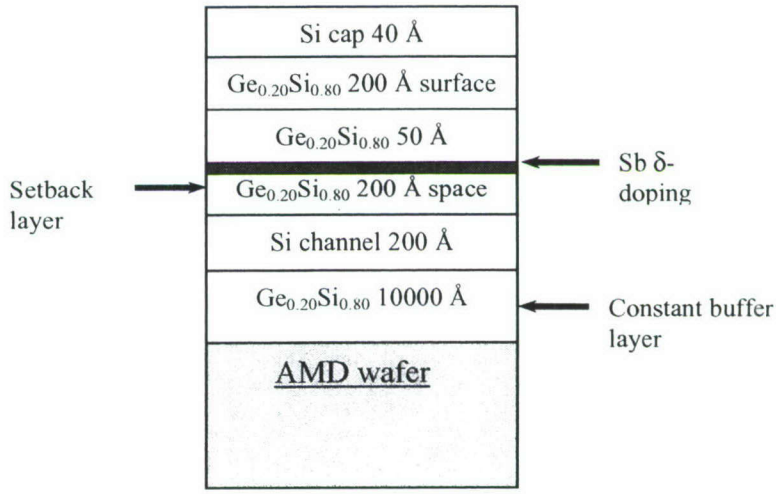

Fig. 1. Schematic of the sample structure

All the samples were grown in a Riber EVA-32 MBE. For $Si_{0.8}Ge_{0.2}$ virtual substrates, they were supplied by Advanced Micro Devices with relaxed $Si_{0.8}Ge_{0.2}$ and graded SiGe buffer layer. The samples were cleaned with modified Piranha method before loaded into the introduction chamber. After transferred into the growth chamber, the samples were heated up to 800 °C for 10 minutes. Then 1 μm constant $Si_{0.8}Ge_{0.2}$ were grown on the virtual substrate, followed by 20 nm Si channel and 20 nm spacer. 1000-second Sb delta-doping concentrations were used and followed by another 20 nm SiGe spacer layer and 4 nm Si capping layer. Figure 2 shows the corresponding longitudinal (ρ_{xx}) and Hall (ρ_{xy}) magnetoresistivities. The electron mobility and density are determined to be 350,000 cm2/V-s and 3.63×10^{11} cm^{-2}, respectively.

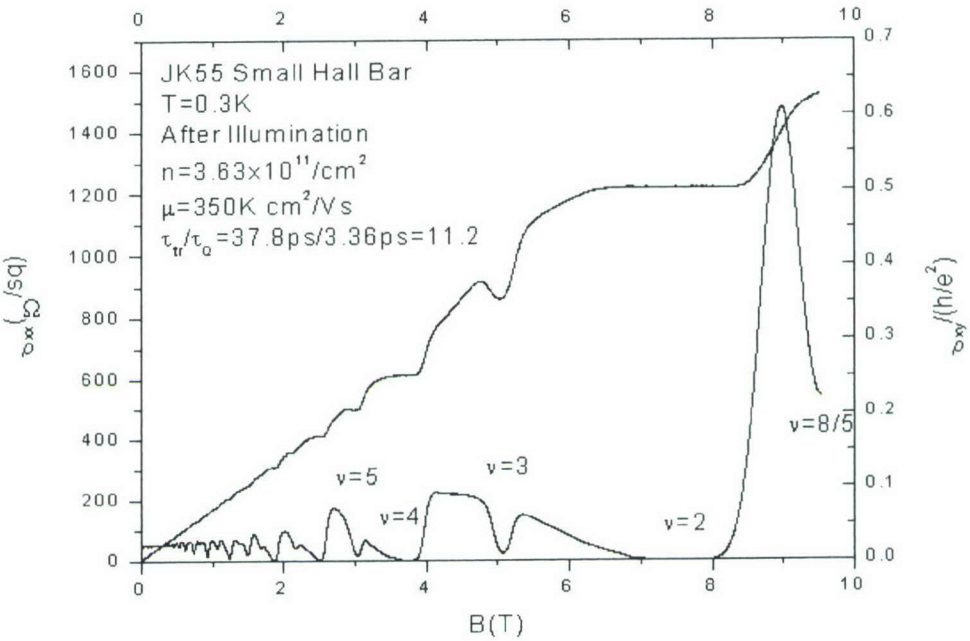

Fig. 2 the longitudinal (ρ_{xx}) and Hall (ρ_{xy}) magnetoresistivities as a function of magnetic field at T=0.3 K after illuminations for the highest mobility sample.

2. The quest for tailoring 2D electron density

Two-dimensional electron gas of strained silicon on SiGe system has been extensively studied since the modulation doping and graded buffer layer have been developed. Besides electron mobility, electron density is another key factor that has been mostly focused on for the strained silicon research. Conventionally, Doping concentration, setback layer thickness (referred to the layer between the doping region and the channel region, in our case, it is shown in Fig.1) and gated structures are used to change the electron density in the strained silicon channel. However, the well-known tendency of Sb surface segregation during Si MBE growths makes precision control of the doping concentration difficult; the reduction of setback layer usually results in low electron mobility due to the remote impurities scattering from the dopant; gated structures still have some problems, such as oxide leakage, source-drain contact, etc. A new approach to tune the electron density will benefit the research for 2DES transport.

We demonstrate the tuning of electron density by changing the distance the re-growth interface and the 2DES layer in 2DES in strained channel of a Si/SiGe heterostructure. Because of p-type substrate used in the experiment, the Fermi level at the re-growth interface was pinned at the band edge of the valence band at low temperature, however, it was touching the conduction band minimum at 2DES layer. Therefore, the electron density can be tuned by

the "level length" between these two pinpoints in the band alignment. In this letter, the distance was varied by different SiGe constant buffer layer thicknesses, which is shown in Fig. 1. Theoretical simulations consistent with experimental results were showing that the electron density could be changed as a function of different buffer layer thicknesses.

Figure 3 shows the sheet electron density at 0.3K as a function of $Si_{0.8}Ge_{0.2}$ constant buffer layer thickness. It is worth noting that the electron density can be tuned from 2.2×10^{11} /cm^2 to 3.5×10^{11} /cm^2 while the buffer layer thickness is increasing from 200 nm to 1000 nm. It is very interesting to further explore the physical mechanisms by calculation of band diagram and electron density at low temperature. The numerical simulations are done by solving the Poisson equation and Schördinger equation self-consistently. The temperature is set to be 0.3K. The Fermi level at the surface is assumed to be pinned in the middle of the band gap because of the severe surface state. The Fermi level at the substrate interface is fixed at the band edge of valence band because the p-type substrate is intentionally used. The substrate doping concentration is set to be 1×10^{18} /cm^3, which was determined by spreading resistance analysis (SRA). The conduction band minimum at quantum well region is just touching the Fermi level because the electrons are transferred from n-type dopant region into the quantum well region. So there are three fixed points in the conduction band diagram at such a low temperature. The carrier density is tuned by the level length from the fixed point at the substrate interface and the fixed point at quantum well minimum. The distance is varied by the $Si_{0.8}Ge_{0.2}$ constant buffer layer thickness. As the buffer layer is thinning down, which means the conduction-band fixed point at the substrate interface is getting close to the quantum well minimum. So the quantum well region will be lifted up higher and the electron in the strained silicon will be less. The detailed conduction band diagram is shown in the inset of Figure 4. It simulates the conduction band diagram and electron density for sample structure with 225 nm buffer layer.

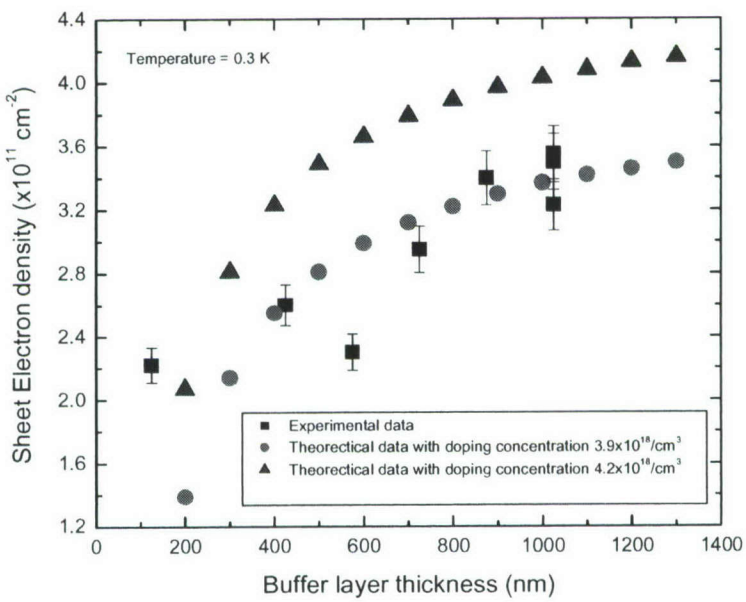

Figure 3. Theoretical simulations and experimental results for the relationship between the electron density in the quantum well and the constant composition $Si_{0.8}Ge_{0.2}$ buffer layer thickness.

The round spots in Figure 3 show the calculated sheet electron density in the quantum well region as a function of constant buffer layer thickness for a doping concentration 3.9×10^{18} /cm^3 at low temperature. It is assumed that all the donors are all ionized at 0.3K. The electron density from the donors are confirmed by SRA measurement. The square spots are the experimental results determined from Shubnikov-de Haas oscillations at 0.3K. From Figure 3, it can be seen that the electron density is increasing with the buffer layer thickness increases. The experimental results are quite consistent with the theoretical simulations. The buffer layer thickness can be used as a structure factor to control the electron density in the quantum well. Slightly data deviations from simulations are coming from slightly varied doping concentration. The triangular spots shown in Figure 3 are the calculated sheet electron density for a slightly larger doping concentration of 4.2×10^{18} /cm^3. Compared with the previous calculated electron density for a concentration of 3.9×10^{18} /cm^3, it can be seen that the electron density could change 49% with the doping variation only just 7.7%. The slight change of Sb vapor pressure is due to 0.8-degree temperature change in Sb dopant source, which is most likely in our case. It has been shown that most of experimental data are consistent with the theoretical simulations, which indicates the rather repeatable doping profile controls in the process.

The differentiation of the electron density can be seen in Figure 4 as a function of the buffer layer thickness. It is shown that when the constant buffer layer thickness is larger than 1000 nm, there is no remarkable change in electron density. The electron density will saturate as the buffer layer thickness increases. The further apart the quantum well separates from the substrate interface, the less impact on the electron density the interface impurities will have. However, when the constant buffer layer thickness is less than 200 nm, the conduction band minimum is just barely touching the Fermi level. Slightly change of the buffer layer thickness will have great influence on the electron density in the well. And also for the buffer layer thickness less than 200 nm, the electron density will be less than 1.3×10^{11} cm^{-2}, which could be localized by the deformation potential undulation caused from strain undulation just below the Si channel. Then there will be no existing free electron gas for the Hall measurement.

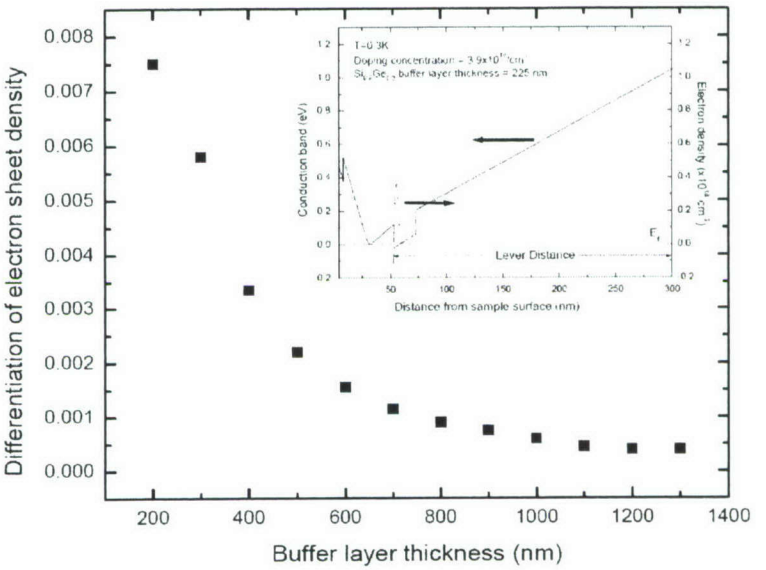

Figure 4. Differentiation of the electron density as a function of the re-grown constant composition $Si_{0.8}Ge_{0.2}$ buffer layer thickness.
Inset: Simulations of the Conduction band diagram and electron density in the quantum well for a 225 nm $Si_{0.8}Ge_{0.2}$ buffer layer structure.

(2) Apply the strain in the thin Si layer by using porous silicon and compliant substrate

1. Fabrication of dislocation-free strained Si layer using oxidation of thin Si on porous Si substrate

For the study of two-dimensional electron gas in strained Si, compositionally graded SiGe buffer has been employed since it reduces threading and misfit dislocation density. However strain field from remaining misfit dislocation causes strain undulation at the strained Si layer. For low temperature quantum transport study, this is serious concern in that the strain undulation causes potential undulation in the strained Si layer which limits low temperature carrier transport. In order to resolve aforementioned problems, we developed the method to fabricate strained Si which is not including dislocation in all process steps. We employ a self-limiting process to fabricate thin Si films as thin as 100 nm on porous Si substrate of several hundred micrometer thickness. Low temperature

oxidation of the porous Si substrate results in thin Si film being strained to as high as 1% via expansion of porous Si substrate, comparable to that in a Si film epitaxially grown on a relaxed SiGe buffer layer of 25% Ge content.

Intrinsic Si layers of various thicknesses (100nm~400nm) are grown on top of the heavily doped p-type substrate using a molecular-beam epitaxy (MBE) system. The anodization is performed for 4 hrs with a current density of 50mA/cm^2 in an electrolyte composed of 1:1 volume ratio of HF (49%) to ethanol. The anodization comes to a nearly complete stop when the anodization front reaches the intrinsic Si layer. The anodized samples are oxidized at 500°C in a steam ambient with 20 sccm O_2 flowing through the boiling deionized (DI) water. The strain increases linearly with increasing oxidation time until it reaches saturation at a critical value. Figure 5 shows the dependence of strain in the thin Si film on the oxidation time. We consider the universal behavior of films of various thicknesses for short oxidation times to be a result of the fact that they are fully strained. The critical strain value is higher for thinner Si layers, being approximately 1.0%, 0.6%, and 0.4% for the Si layers of 100 nm, 200 nm and 400 nm, respectively. Considering the tensile nature of the strained thin Si layers, the observed strain saturation may be the result of crack formation or a combination of dislocation and crack formation.

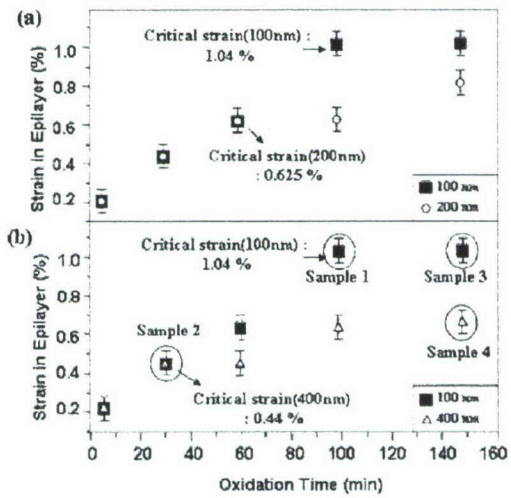

Figure 5. Strain in the thin Si films as a function of oxidation time. (a) The 100 and 200 nm thick Si films, and (b) the 100 and 400 nm thick Si films.

We performed defect etch on the samples before and after strain relaxation For the samples with 100nm and 400nm Si thickness (marked as sample 1 and sample 2 respectively in Figure 5 (b)) oxidized right before strain saturation, cracks and etch pits are absent under both the optical microscope and SEM. This result clearly indicates that the layers whose strains are in the linear regime in Figure 1 have neither dislocation nor crack. This is a significant step forward in sample fabrication for transport physics research into 2DES under extreme conditions. On the other hand, Figure 6(a) and (b) show that there are crack but not etch pits in the 100nm Si layer oxidized for 150 min (sample 3), which is during the early stage of relaxation. For thicker films (e.g. sample 4 with 400 nm Si thickness) whose misfit and residual strains are higher than critical strain for dislocation introduction, Figure 6(c) and (d) show clear signs of both cracks as well as

dislocations (as evidenced by the presence of etch pits). The strain confirmed via multiple strain measurements via Raman spectrometer across the fully strained 100 nm sample shows that the strain is uniform within the experimental uncertainty (<1 cm^{-1}) of the Raman technique.

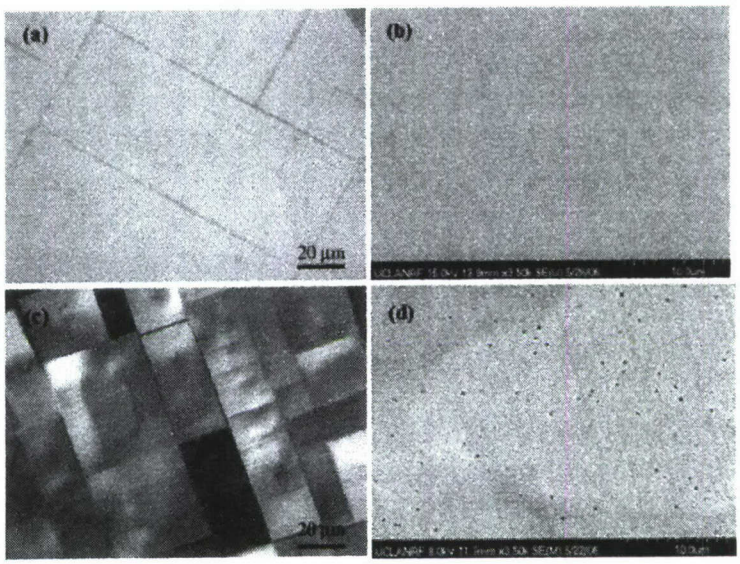

Figure 6. Plan-view micrographs from relaxed layers after defect etch. (a) The Nomarsky interference micrograph of the 100 nm thick Si (sample 3) and (b) the SEM micrograph of the 100 nm thick Si (sample 3). (c)The Nomarsky interference micrograph of the 400 nm thick Si(sample 4) and (d) the SEM micrograph of the 400 nm thick Si (sample 4).

2. Fabrication of uniaxially strained dislocation-free strained Si layer

Recently, experimental results show that uniaixal strain leads to significant enhancement in carrier mobility than biaxial strain, where hole mobility is increased by compressive strain and electron mobility is increased by tensile strain. Maximum enhancement has been shown by uniaxial deformation along the <100> direction for electrons and along <110> direction for holes. Therfore uniaxial tensile strain along <100> can enhance electron transport in 2DES. We develop the method to induce uniaxial strain in strained Si layer without dislocation introduction through oxidation of selectively anodized porous Si substrate. In general, the micro-porous Si is produced via anodization of a heavily doped p-type wafer in an electrolyte composed of typically 1:1 volume ratio of HF 49% to ethanol. The center part of a wafer can be selectively anodized by controlling an exposed area to HF-ethanol solution. The expansion of the porous Si via oxidation can be restricted by the rigid edge of bulk Si surrounding the porous Si. The direction of expansion is controllable by preferentially removing this rigid edge of bulk Si around the porous Si region. While dicing every four sides of edges allows biaxial strain upon oxidation, removing only two opposite sides of edges allows unaxial strain to be achieved upon oxidation. The magnitude of strain, of course, can be controlled by the oxidation time. Figure 7 shows schematics of this procedure.

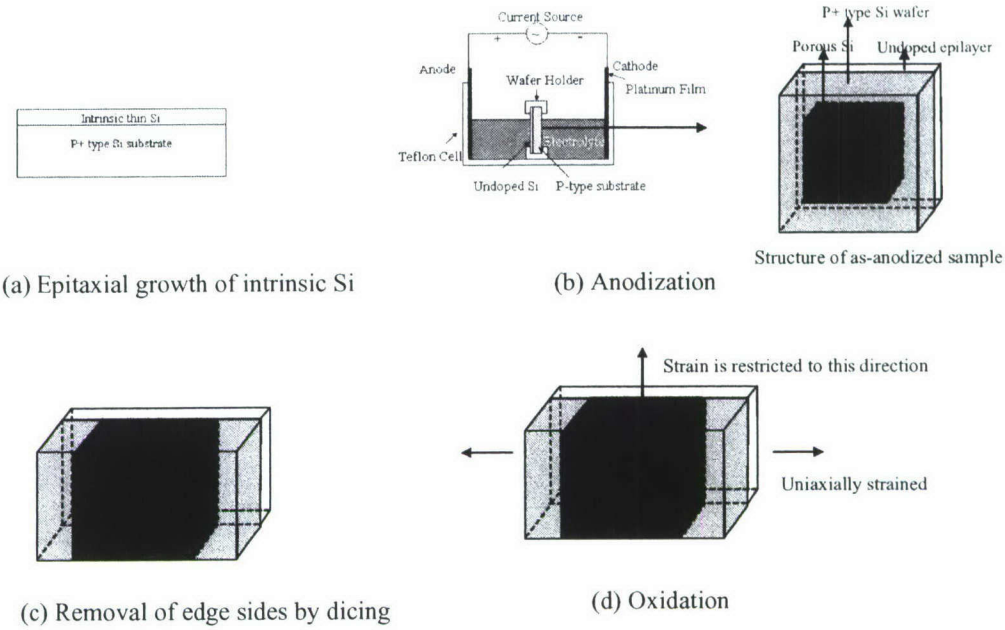

Figure 7. Schematics of process to apply uniaxial strain to the thin Si layer

The strain level after the oxidation is measured using Raman spectrometer. The biaxial and uniaxial strained samples are simultaneous fabricated and strain levels are compared. Since Raman shift of the strained sample is originated from two dimensional signal, Raman shift from uniaxially strained Si must be half of the shift from biaixally strained Si. Our experimental result follows this rule showing that this method is promising to fabricate uniaxially strained Si layer.

3. 2DES structures on porous Si substrate

The porous Si substrate cannot be used as a substrate for further epitaxial growth because stress condition of porous Si can be easily changed by any other heating step, for example in-situ oxide desorption process during MBE growth. The strained film on the porous Si substrate can be bonded to a Si substrate covered with SiO_2 to form strained Si on insulator (SSOI), then Si/Ge heterostructure for 2DES can be epitaxially grown on SSOI. However, there exists uncertainty to succeed in this process due to rough surface after anodization and wafer bowing from the stress evolution in the wafer after oxidation. Alternatively, Si/Ge heterostructre for 2DES can be grown on a heavily doped p-type substrate before anodization. Intrinsic or n-type Si can be placed between Si/Ge heterostructure and substrate as an anodization stop layer. Then this structure can be strained after anodization by oxidation. Figure 8 shows schematics of this procedure

This structure is oxidized at 500°C until the strain level in the strained Si reaches to 0.8% strain, which is a desired strain level for 2DES. The characteristics of low temperature electron transport in this sample are under investigation.

Future plan for fabricating dislocation-free strained Si films

1. The effect of strain undulation from misfit dislocation on the minimum achievable carrier density in 2DES structure should be studied by dislocation simulation and experimental measurement.

2. Electron transport in the 2DES structure on the porous Si substrate should be investigated in detail

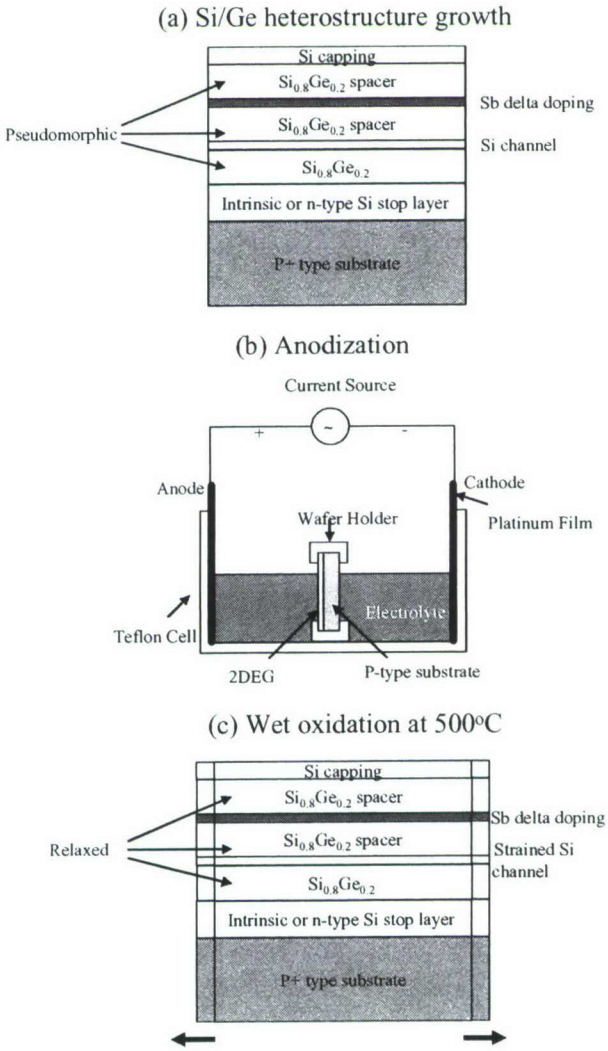

Figure 8. Schematic illustration of the process in which to fabricate the 2DES on the porous Si substrate.

(3) Low-dimensional physics study by Princeton University

1. Valley splitting of n-Si/SiGe heterostructures in tilted magnetic fields

The study of the valley splitting (Δ) of two-dimensional (2D) electrons confined in n-type Si/SiGe heterostructures has been highlighted by recent research efforts on Si-based quantum computation. In a single-particle picture, the surface electric field breaks the symmetry of the two out-of-plane valleys, resulting in an energy splitting proportional to the electron density. The many-body interaction, on the other hand, also affects Δ and this effect is not fully understood, especially in the presence of strong perpendicular magnetic fields.

Seven modulation doped n-Si/SiGe heterostructures were investigated in our study, with the densities (n) ranging from 1.4 to $3.1\times10^{11}cm^{-2}$ and mobility (μ) from 6.3 to $25m^2/Vs$. The experiments were carried out in the 18/20T superconducting magnet cell and the 35T resistive magnet cell, both equipped with a top-loading dilution refrigerator. The high field and low temperature facilities enabled us to access the valley-split states up to very high tilt angles.

We studied the $\nu=3$ energy gap at various tilt angles by measuring the thermal activation of the transport coefficient. Our previous tilted-field experiments were performed near the coincidence angles, where the inter-valley energy gaps exhibit an anomalous rise toward the coincidence angle. Here we focus on tilt angles away from the coincidence, at which the strength of the valley-split states does not change with the parallel field component. For all seven samples, the valley splitting at the $\nu=3$ state after the coincidence (Δ_{3A}) is significantly bigger than that before the coincidence (Δ_{3B}). Both Δ_{3A} and Δ_{3B} show linear dependence on the electron density, while the slope of these two configurations differs by more than a factor of 2.

The difference between Δ_{3A} and Δ_{3B} can be explained as follows. Before the coincidence, the spin-up low-lying electrons can approach the spin-down electrons at the Fermi level (E_F) and strongly screen the Coulomb interaction. The many-body enhancement is thus much reduced. On the other side of the coincidence, such screening is less effective since the low-lying electrons and the electrons at EF belong to different Landau levels with the same spin, resulting in a bigger Δ.

Our results reveal very interesting physics on the valley splitting in Si 2D electrons. Out of the coincidence region, the splitting only depends on the perpendicular field, while it differs significantly for different Landau or spin levels. We propose that screening of the Coulomb interaction from low-lying filled levels could be responsible for this difference.

2. Capacitively induced high mobility two-dimensional electron gas in undoped $Si/Si_{1-x}Ge_x$ heterostructures with atomic-layer-deposited dielectric

Modulation-doping and the SiGe virtual substrate technique have enabled the realization of high mobility 2DESs in $Si/Si_{1-x}Ge_x$ heterostructures. However, the mobility is limited by the remote dopants at very low temperature. A MOSFET-like heterostructure with no intentional dopants has the potential of achieving extremely high mobility. We

successfully fabricated an undoped $Si/Si_{1-x}Ge_x$ heterostructure FET, using atomic-layer-deposited Al_2O_3 as the dielectric.

The device structure is shown in Fig. 9. The relaxed buffer of the virtual substrate had 20% Ge content. The virtual substrate was loaded into the molecular-beam-epitaxy (MBE) chamber after a modified Piranha clean was performed. A 1μm relaxed $Si_{0.8}Ge_{0.2}$ buffer was grown first, followed by a 100 Å strained Si channel and a 450 Å $Si_{0.8}Ge_{0.2}$ barrier layer, terminated with a 40 Å Si cap. After removing the sample from the MBE chamber, a Piranha clean was performed, and 50 Å /1000 Å Au/AuSb was deposited to form the contacts around a 400μm x 400 μm van der Pauw square. The sample was then annealed in forming gas (90% Nitrogen + 10% Hydrogen) for 10 minutes at 400°C, which was the highest temperature the sample experienced after the MBE growth. One thousand cycles of ALD Al_2O_3 about 1100 Å thick, were deposited at 150°C to cover the top surface. The Al_2O_3 works as both the gate dielectric and the insulator between the contacts and the gate. Trimethylaluminum and water were used as the precursors. Finally, 50 Å /2000 Å Ti/Au was deposited as the gate, defined by photolithography.

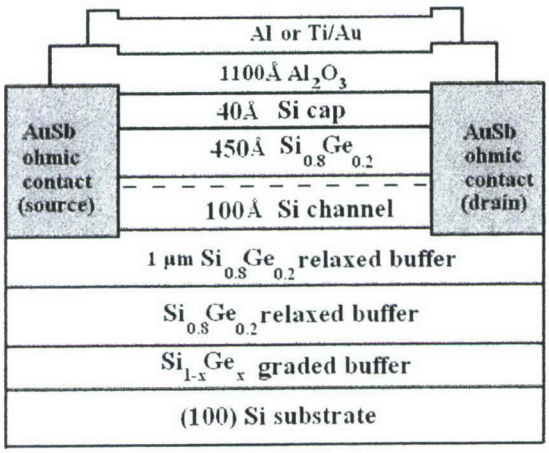

Fig.9 Schematic view of the device structure. The dashed line denotes the capacitively induced 2D electrons in the channel.

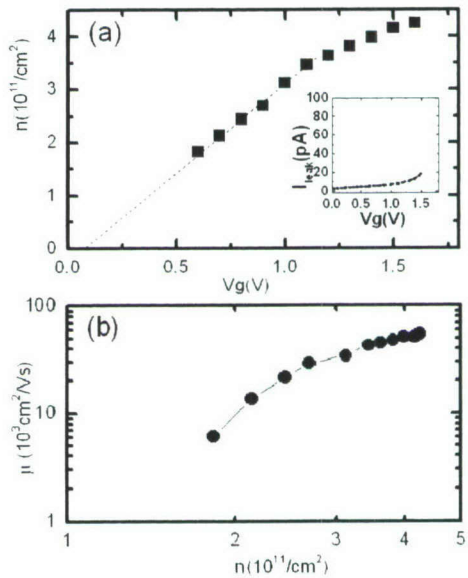

Fig.10 (a)n vs. Vg measured at T=0.3K. The density is determined from the Shubnikov-de Haas oscillations in R_{xx}. The dependence is extrapolated to n=0, as shown by the dotted line. Inset: The gate leakage current vs. Vg. (b)μ as a function of n.

The density (n) of the 2DES, determined from the Shubnikov-de Haas oscillations, is shown as a function of the gate voltage (Vg) in Fig.10(a). At Vg>0.6V, well defined quantum oscillations allow for precise determination of n. For 0.6V<Vg<1.1V and 1.1V<Vg<1.7V, n is linearly dependent on Vg, with effective capacitance C_{eff} of 52 nF/cm^2 and 26 nF/cm^2, respectively. The highest achievable density is $4.2x10^{11}$/cm^2, limited by the increase in gate leakage current, as shown in the inset of Fig. 10(a). The

ideal capacitance derived from the parallel capacitor model is 55 nF/cm^2, consistent with C_{eff} observed experimentally for $0.6V<Vg<1.1V$. Figure 10(b) shows the mobility μ as a function of n. μ first grows rapidly with n, and then increases at a slower rate at high densities. The highest achievable mobility is $5.5x10^4$ cm^2/Vs, comparable to the mobility of the modulation-doped heterostructures grown in the same run. Thus, the dominant disorder is likely the unintentional background impurities. At low densities, μ decreases very rapidly with decreasing n, possibly insinuating the breakdown of screening of the background disorder, consistent with the percolation picture.

Figure 11 shows R_{xx} (upper panel) and R_{xy} (lower panel) as a function of magnetic field (B) at 3 different densities. Well quantized plateaus in R_{xy} and vanishing minima in R_{xx} at integer filling factors prove the high quality of the 2DES. As n increases, more and more plateaus in R_{xy} and corresponding minima in R_{xx} develop, due to improved mobility. At $3.5x10^{11}/cm^2$, the Shubnikov-de Haas oscillations start at B=0.35T with a four-fold Landau level degeneracy, two from spin and two from valley. The spin degeneracy is resolved at B=1.4T. The weak dip near filling factor υ=5 and the strong minimum at υ =3 show that the two-fold valley degeneracy is also lifted at higher B.

The temperature dependence of the zero field resistivity (ρ) at several densities is shown in Fig. 12. At $n>1.9x10^{11}/cm^2$, $d\rho/dT$ is positive, while At $n<1.9x10^{11}/cm^2$, $d\rho/dT$ in the low temperature is negative. An apparent MIT is observed, with a critical density (n_C) of roughly $1.9x10^{11}/cm^2$. The n_C and the resistivity at n_C (ρ_C) are close to the values observed in a modulation-doped Si/Si1-xGex heterostructure of comparable mobility\citeLai2. However, n_C is larger than the values reported for Si MOSFETs and ultra high quality modulation-doped $Si/Si_{1-x}Ge_x$ heterostructures. ρ_C is also much smaller than the quantum resistance (h/e^2). These facts suggest that the relevant physics is classical percolation, in which the 2DES becomes nonuniform at low density and eventually breaks down into puddles of electrons.

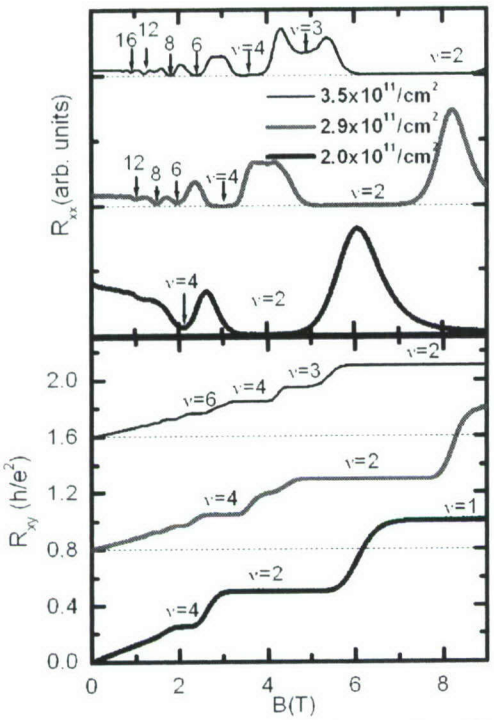

Fig. 11 R_{xx} and R_{xy} at different densities at T=0.3K. Curves are shifted vertically for clarity. The dotted lines show the baseline for each trace.

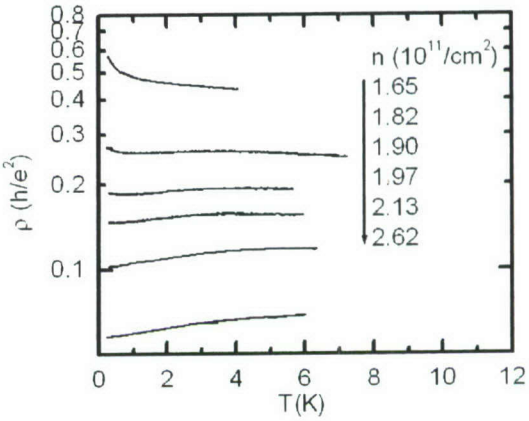

Fig. 12 Temperature dependence of the resistivity at different densities. An apparent MIT is observed near $n=1.9x10^{11}/cm^2$

Future Plan for low-dimensional physics study

1. Due to their super-high mobilities, undoped Si/SiGe FETs should be used to study the 2D Metal-Insulator-Transition.

2. Undoped Si/SiGe nanostructures should be fabricated using the ALD technique described above. The two well-known problems, gate leakage using metallic Schottky gates and damage to the 2DES when etching is employed, are circumvented in this scheme. Thus, the main features of mesoscopic structures in electrical transport, such as quantized conductance, Coulomb blockade, and the Ahanorov-Bohm Effect, are expected to be more well-developed.

Publications

[1] Jeehwan Kim and Ya-Hong Xie, "The fabrication of dislocation-free tensile strained Si thin films using controllably oxidized porous Si substrates", Applied Physics Letters, Vol 89, No 15, 152117 (2006)

[2] Jeehwan Kim, Jae Young Lee, and Ya-Hong Xie, "Fabrication of a strained Si with a uniaxial tension using oxidation of a porous Si substrate", submitted to Appl. Phys. Lett.

[3] J. Liu, T. M. Lu, J. Kim, K. Lai, D. C. Tsui, and Y. H. Xie, "The proximity effect of the re-growth interface on two-dimensional electron density in strained Si", to appear in Appl. Phys. Lett.

[4] T.M. Lu, J. Liu, J.H. Kim, K. Lai, D.C. Tsui, and Y.H. Xie, "Capacitively induced high mobility two-dimensional electron gas in undoped Si/Si1−*x*Ge*x* heterostructures with atomic-layer-deposited dielectric", Appl. Phys. Lett., v.90, 182114 (2007).

[5] J. Liu, J.H. Kim, Y. H. Xie, T. M. Lu, K. Lai, and D. C. Tsui, "Epitaxial growth of two-dimensional electron gas (2DEG) in strained silicon for research on ultra-low energy electronic processes", to appear in Thin Solid Films;

[6] US Patent application filed on July 19, 2005: "Method for fabricating dislocation-free stressed thin films", JeeHwan Kim and Y. H. Xie (Application # : 60/700,448)

[7] US Patent application published on January 25, 2007: "Method of forming dislocation-free strained thin films", JeeHwan Kim and Y. H. Xie (Publication #: US2007/0017438 A1)

[8] US Patent submitted on January 1, 2007: "A Method for Manufacturing of Dislocation-Free Uniaxially Strained Si Thin Films Method for fabricating dislocation-free stressed thin films", JeeHwan Kim and Y. H. Xie (UCLA Case No. 2007-353)

[9] Lai K, Lu TM, Pan W, Tsui DC, Lyon S, Liu J, Xie YH, Muhlberger M, Schaffler F, "Valley splitting of $Si/Si_{1-x}Ge_x$ heterostructures in tilted magnetic fields, Physical Review B, 73 (16) 161301, 2006.

[10] "Intervalley Gap Anomaly of Two-Dimensional Electrons in Silicon", K. Lai, W. Pan, D. C. Tsui, S. Lyon, M. Mu¨hlberger, and F. Schaffler, Phys. Rev. Lett., **96,** 076805 (2006);

[11] "Surface Roughness and Dislocation Distribution in Compositionally Graded Relaxed SiGe Buffer Layer with Inserted Strained Si Layers", T.S. Yoon, J. Liu, A. Noori, M.S. Goorsky, and Y.H. Xie, Appl. Phys. Lett., vol. 87, 012104 (2005);

[12] "Modulation of the high mobility two-dimensional electrons in Si/SiGe using atomic-layer-deposited gate dielectric", K. Lai, P.D. Ye, W. Pan, D.C. Tsui, S.A. Lyon, M. Muhlberger, and F. Schaffler, arXiv:cond-mat/0504484 v1;

Conference Presentations:

"Investigation of upper and lower limits of carrier concentration for two-dimensional electron gas in strained silicon", Jian Liu, Bin Shi, Keji Lai, Tzu-Ming Lu, Ya-Hong Xie and Danie C. Tsui, Internat. SiGe Techn. Dev. Meeting, Princeton, NJ, May 15-17, 2006.

"Surface Roughness and Dislocation Distribution in Compositionally Graded Relaxed SiGe Buffer Layer with Inserted Strained Si Layers", Tae-Sik Yoon, Jian Liu, and Ya-Hong Xie, 2005 APS March Meeting; 3/21-3/25/2005; Los Angeles, CA